ELSEVIER

Materials Characterization 47 (2001) 119–127

MATERIALS CHARACTERIZATION

Ferritic steels
Optimization of hot-rolled textures through cold rolling and annealing

J. Asensio[a,*], G. Romano[a], V.J. Martinez[b], J.I. Verdeja[a], J.A. Pero-Sanz[c]

[a]*School of Mines, University of Oviedo, Oviedo, Asturias, Spain*
[b]*Lloyd's Register, Gijon, Asturias, Spain*
[c]*School of Mines, Polytechnic University of Madrid, Madrid, Spain*

Received 24 October 2000; accepted 30 June 2001

Abstract

This paper describes the processes used in the production of tinplate, autobody and interstitial-free (IF) steels, and examines how the microstructure and the texture of the hot-rolled stock modify the cold formability properties (n, r_m and Δr) of the blanks through the subsequent cold-rolling and annealing processes. The process of fabrication of ferritic steel strip must comply with the specified drawing quality requirements: commercial quality (CQ), drawing quality (DQ), deep drawing quality (DDQ) or extra deep drawing quality (EDDQ). The quality level is determined by several factors, such as the chemical composition, microstructure and texture of the hot-rolled sheet, the percentage of cold reduction (CR) and the recrystallization treatment in the continuous annealing process or batch process. To a lesser degree, other parameters such as the coiling temperature in the hot strip workshop and the degree of reduction in the temper rolling (TR) mill also modify the cold workability of the strip.

Keywords: Ferritic steels; Texture analysis; Microstructure correlations; Hot rolling; Cold rolling

1. Introduction

Sheet steel in either the precoated or the bare state is the preeminent material in the consumer goods industry worldwide and is used extensively in the automotive, canmaking and other transforming industries. The process of fabrication of ferritic steel strip for these applications must comply with the drawing quality requirements contained in the final specifications, i.e., commercial quality (CQ), drawing quality (DQ), deep drawing quality (DDQ), or extra deep drawing quality (EDDQ). Importantly, for good cold formability, the steel must have the following characteristics [1]:

- high r_m value (mean normal anisotropy coefficient),
- high n value (work hardening index),
- low Δr value (planar anisotropy coefficient or "earing" parameter), which determines the metal yield after sheet metal drawing.

* Corresponding author. Departamento de Ciencia de los Materiales (Siderurgia), E.T.S. de Ingenieros de Minas, C/Independencia, 13, 33004 Oviedo, Spain. Tel.: +34-985-104302; fax: +34-985-104242.
E-mail address: jasensio@etsino.uniovi.es (J. Asensio).

1044-5803/01/$ – see front matter
PII: S1044-5803(01)00160-7

The value of r_m, in particular, dictates the quality category of the steel:

CQ	$r_m = 1$
DQ	$r_m = 1.1 - 1.3$
DDQ	$1.5 < r_m < 2$
EDDQ	$r_m > 2$

All three of the above parameters can be derived in metallic materials from a simple tensile test and, thus, the ductility of the material can be precisely determined. In addition, they can be used to predict the formability when strip cuts are subjected to complex stress–strain states, such as those that occur during deep drawing processes.

Standard sheet drawing tests subject the material to deformations that closely reflect the particularly complex stress distributions found in the industrial forming operations. These can be classified based on which of the major types of cold deformation processes takes place, i.e., bending, stretching, drawing or stretch drawing. Perhaps the most severe and complex test refers to the last two types of deformation mechanisms, and among the many variants of such tests, the most popular are the Swift flat-bottomed cup test and the Erichsen cup test. The Swift flat-bottomed cup test evaluates a material's ability to contract in the plane of the sheet to flow into a hole of standard dimensions. The hemispherical punch test (Erichsen cupping test) evaluates the capacity of the material for expanding by stretching. Forming limit diagrams serve to validate the intermediate complex situations that can take place during industrial sheet metal forming and underline the importance and simplicity of the three parameters mentioned above: r_m, n and Δr.

Grain orientation has a strong influence over r_m and Δr in cold-formed and annealed sheet steel because of the direct relationships that exist between both parameters and the crystallographic texture of the steel. Texture characterization techniques utilize physical references such as the rolling direction and the rolling plane to establish a set of orthogonal axes [longitudinal direction (LD), normal direction (ND) and transverse direction (TD)] in order to uniquely identify the crystalline directions $\langle hkl \rangle$ and planes $\{hkl\}$. On the other hand, the n value is primarily influenced by the chemical composition and the presence of second-phase particles, and only secondarily by the grain size [2].

To the target of high formability should be added the need for a smooth surface quality, a very precise thickness and a uniform flatness profile in the finished product. An emblematic product is the double-reduced tinplate. By virtue of its higher strength, double-reduced tinplate provides the ability to reduce the cost of a can or other components by permitting a decrease in the thickness of the material without a loss of rigidity. However, these materials exhibit a marked directionality in properties [3]. The strip width tolerances must be in the range 0–3 mm, the thickness within 8.5% of the nominal value, for a product with thickness varying between 0.13 and 0.29 mm. For the automotive industry, the cold-rolled sheet steel dimensional tolerances are specified in UNE 36-563 standards: the width tolerance should be in the range 0–4 mm and the thickness tolerance within 0.08 mm for a 0.61- to 0.70-mm-thick strip. With reference to the surface quality, the "Z-finish" usually specifies that one side of the sheet must bear no defects in order to assure a uniform appearance after painting or electrolytic coating. The limitations also extend to the surface roughness, which affects the phosphating and painting posttreatments. For this reason, it is recommended that profiles have considerable emptying degrees, tall peaks, deep valleys and more than 135 peaks per inch (EuroNorm 49/72).

The production route of ferritic steel strip is somewhat complex, comprising several steps, each of which plays a role in the formability of the cold-rolled and annealed sheet. In addition, because of the increasing overall demand for these steels, which account for tens of millions of tons per year, more and more stringent compositional limits have been added to the automotive and the canmaker standards to guarantee the homogeneity of their products. The quality of the final product is linked to the use of in-plant generated scraps with the ever increasing restrictions on residual elements. Among others, dissolved P and S must be kept below certain limits such as those in the present three experimental steels.

The majority of the total output of ferritic steels is processed through the integer route, i.e., blast furnace followed by steel-making processes. Pig iron is the result of the coke reduction of the iron oxide burden in the blast furnace. Thereafter, decarburization in the oxyconverter furnace drops the C content to 0.05% at the end-blow. Degassing processes follow through Ar blowing and high vacuum.

Table 1
Properties of ferritic steels for drawing operations

Steel type	σ_y (MPa)	UTS (MPa)	Elongation (%)	n	r_m
Interstitial-free	155	305	42	0.23	2.0
Al-killed	165–190	300	42	0.22	1.8
Rephosphorized	190–230	345–370	36	0.20	1.5
Bake-hardened	210	320	40	0.22	1.6
HSLA	375	475	27	0.15	1.0

Table 2
Chemical composition of the experimental materials (in wt.%)

Steel identification	C	Mn	Si	S	P	N	Al	Others
Tinplate	0.08	0.4	<0.1	<0.03	<0.03	<0.004	0.06	–
Autobody	0.05	0.25	<0.1	<0.03	<0.03	<0.004	0.04	–
Interstitial-free	0.0023	0.126	0.01	0.004	0.009	0.004	0.03	0.05% Ti, 0.002%Nb, 0.002% V

Further treatment in the secondary steel-making units permits the removal of metalloids and the final adjustment of the composition to meet the customer's demands.

Table 1 summarizes the mechanical properties and drawing parameters of the five basic ferritic steel categories for cold formability: interstitial-free (IF), aluminum-killed, rephosphorized, bake-hardened and microalloyed (HSLA) steels. It will be noted that their respective r_m values set them in different formability categories.

With the above in mind, it was decided to perform a characterization of the processes used in the production of tinplate, autobody and IF steels, with a view to assessing their formability properties. The principal foci of the characterization were the steel microstructure and texture following each stage in the production process, from the initial hot rolling through the cold-rolling stage and into the final annealing stage.

2. Experimental material and techniques

Careful control of the carbon level must be adopted because of its numerous implications, varying from 0.12 to 0.08 wt.% in tinplate, 0.04 wt.% in autobody panels and 0.002 wt.% in the extra-low-carbon steels. In addition, interstitial elements such as H, O, N, P and S must be carefully controlled and monitored [4]. The chemical compositions of the three steels involved in the present investigation are presented in Table 2.

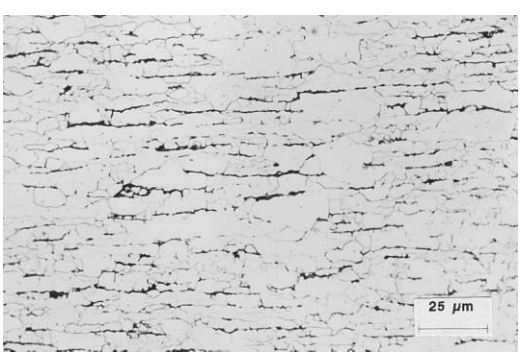

Fig. 1. Microstructure of the tinplate steel in the hot-rolled state. Etchant: 2% Nital.

3. Results

3.1. Hot rolling processing

Hot rolling usually involves a homogenization or soaking treatment at high temperatures followed by a thermomechanical treatment. Typically, it consists of deformation schedules organized in roughing and finishing passes. Of the several parameters to be controlled, the final rolling temperature is perhaps the process variable that has the most effect on the microstructure. The control over the rolling parameters allows the production of the rolling textures most appropriate for the requested DQ. Whether or not the hot-rolling process is performed under controlled

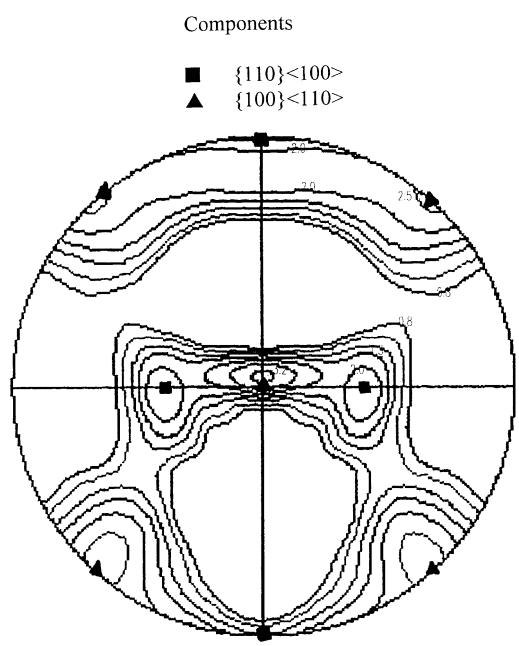

Fig. 2. {200} Pole figure of the tinplate steel in the hot-rolled condition.

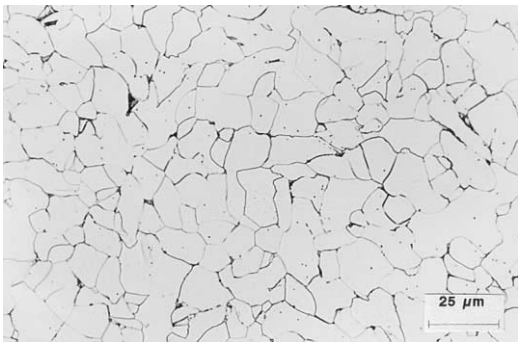

Fig. 3. Microstructure of the autobody steel in the hot-rolled condition. Etchant: 2% Nital.

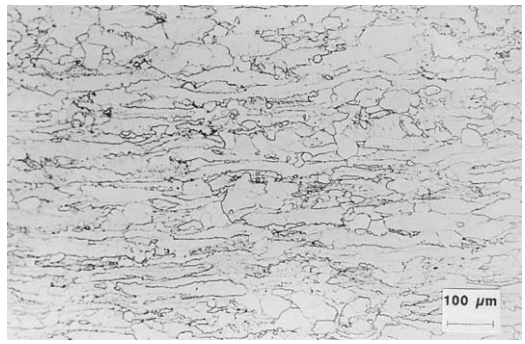

Fig. 5. Microstructure of the IF steel in the hot-rolled condition. Etchant: 2% Nital.

conditions, the texture and the grain morphology of the gamma phase have a "parental" effect on the ferrite grains resulting from the allotropic transformation $\gamma \rightarrow \alpha$. This relation between γ and α grains dictates the specific rolling formulations for the different steel categories produced.

3.1.1. Tinplate steel

For the 0.08% C tinplate packaging steels, "hard" rolling schedules are preferred with finishing passes at temperatures below the no-recrystallization temperature (T_{nr}) of the austenite, but above A_{r3}, the two temperatures being given by the following formulations [5]:

$$T_{nr}\ (^\circ\mathrm{C}) = 887 + 464(\%\mathrm{C}) + [64455(\%\mathrm{Nb}) - 644(\%\mathrm{Nb})^{1/2}] + [732(\%\mathrm{V}) - 230(\%\mathrm{V})^{1/2}] + 890(\%\mathrm{Ti}) + 363(\%\mathrm{Al}) - 357(\%\mathrm{Si})$$

$$A_{r3}\ (^\circ\mathrm{C}) = 910 - 310(\%\mathrm{C}) - 80(\%\mathrm{Mn}) - 20(\%\mathrm{Cu}) - 15(\%\mathrm{Cr}) - 55(\%\mathrm{Ni}) - 80(\%\mathrm{Mo}) + 0.35(t - 8)$$

where t is the strip thickness in millimeters.

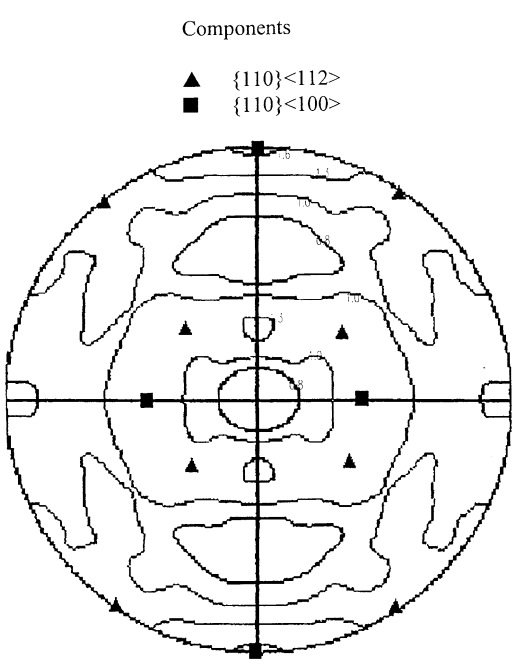

Fig. 4. {200} Pole figure of the autobody steel in the hot-rolled condition.

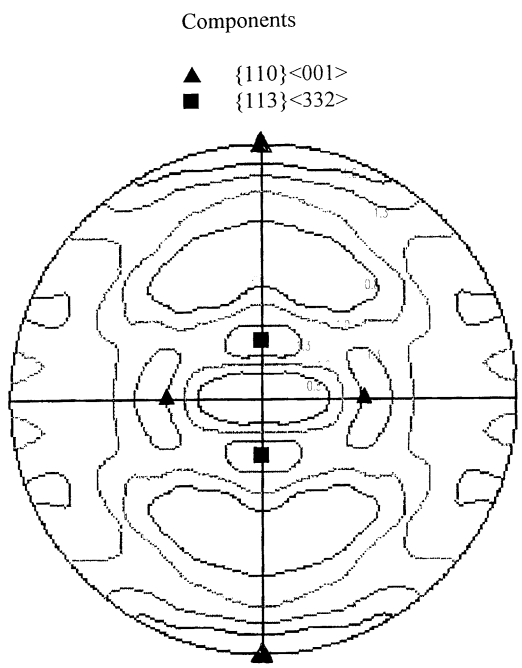

Fig. 6. {200} Pole figure of the IF steel in the hot-rolled condition.

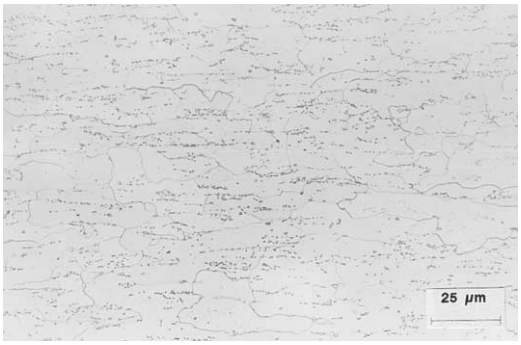

Fig. 7. Microstructure of the tinplate steel in the cold-rolled and annealed condition. Etchant: 2% Nital.

Fig. 9. Microstructure of the autobody steel in the cold-rolled and annealed condition. Etchant: 2% Nital.

Fig. 1 shows the microstructure of the tinplate steel in the hot-rolled state with pearlite banding in much evidence. The measured grain size is ASTM 12. The transformation textures are strongly marked with the crystallographic planes {110} and {100} lying parallel to the rolling plane of the strip (Fig. 2).

3.1.2. Autobody panels

Softer rolling sequences are preferred for the production of automotive sheet panels (0.04% C, DDQ), with finishing passes ending at temperatures equal to or slightly higher than that corresponding to the transformation. The microstructure consists of equiaxed grains (Fig. 3) with grain size equal to ASTM 10. The crystallographic texture is less defined than in the tinplate steel, with {110}⟨112⟩ and {110}⟨100⟩ as the preferred orientations lying in the rolling plane and parallel to the rolling direction, respectively (Fig. 4). This texture is the commonest in ferritic steels.

3.1.3. Instertitial-free steel

IF steels in the range of the EDDQ class are finish-rolled, ending with the last passes in the "soft" α phase. That is, the hot-rolling schedule follows below T_{nr} in phase, and through the allotropic transformation in $(\alpha+\gamma)$ and or α. The microstructure is

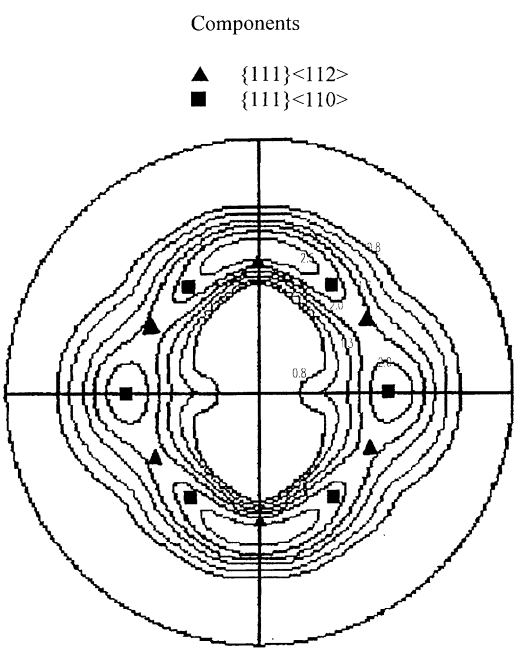

Fig. 8. {200} Pole figure of the tinplate steel in the cold-rolled and annealed condition.

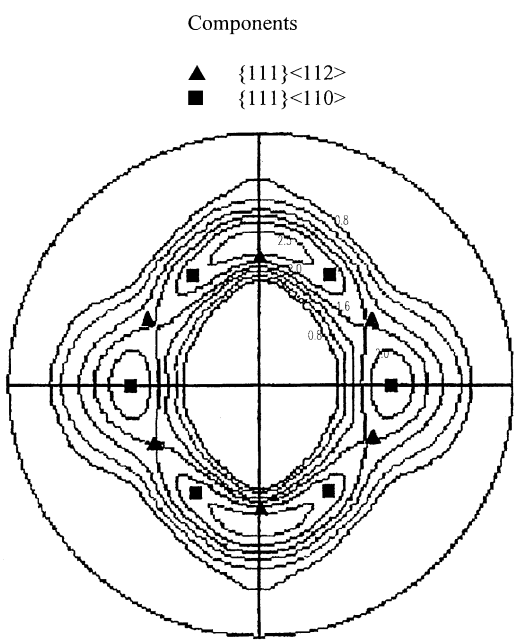

Fig. 10. {200} Pole figure of the autobody steel in the cold-rolled and annealed condition.

Table 3
Principal texture components of an autobody steel after CR and after CR plus batch annealing

	CR		CR and annealing		
			CR = 70%; $T_a(\cdot)$ = 50 °C/h; T_a = 700 °C		CR = 90%; $T_a(\cdot)$ = 50 °C/h; T_a = 700 °C
Texture	CR = 70%	CR = 90%	t_a = 1 h; TR = 1%	t_a = 3 h; TR = 1%	t_a = 3 h; TR = 0%
{001}⟨110⟩	4.99	8.24	–	–	2.10
{001}⟨230⟩	4.00	4.60	–	–	–
{112}⟨110⟩	3.30	7.41	2.13	2.03	2.55
{111}⟨110⟩	3.12	6.54	8.68	9.40	6.98
{111}⟨112⟩	3.93	9.61	5.57	5.07	7.21
{554}⟨225⟩	4.19	7.16	5.75	5.96	6.99

shown in Fig. 5, and its complexity is manifested in the presence of partially recovered and partially recrystallized grains, resulting in heterogeneous grain structures. The crystallographic texture (Fig. 6) is somewhat different from that of the previous material, having a marked Goss texture {110}⟨100⟩ and a less defined {113}⟨332⟩ orientation typical of hot-rolled ferrite in steels, which do not verify the transformation [6].

Another important process variable is the coiling temperature, between 550 and 700 °C. This is linked to the annealing process type that follows the cold rolling of the strip. Continuous annealing processes require higher soaking temperatures for the cast slab and high coiling temperatures. AlN precipitation occurs during the coiling of the strip and reduces the total ductility of the hot-rolled material. On the other hand, it suppresses the amount of interstitial N and therefore inhibits the natural aging process. Sheets processed in the batch annealing plants are coiled at temperatures lower than 600 °C after hot strip rolling and accelerated cooling. This schedule results in a supersaturated solution of Al and N in ferrite, thus avoiding precipitation of AlN. However, precipitation will take place in the heat-up stage during batch annealing, favoring the {111} orientation in the recrystallized grains. Here, the variable is the heating rate, which should not exceed 50 °C/h. The optimum for this variable can be calculated through the following formulation [7]:

$$\log V_{opt} = 18.3 + 2.7\log[(\%Al)(\%N)(\%Mn)/(\%CR)]$$

where V_{opt} is the optimum heating rate, (%Al), (%N) and (%Mn) are the weight percents of the respective elements and (%CR) is the percent of cold reduction (CR) applied in the former stage.

3.2. Cold rolling and recrystallization annealing processing

Hot rolling is followed by the cold-rolling and annealing processes, both of them very important in the determination of the cold formability of the final product. During cold rolling, the strip hardens at increasing work hardening rates for the higher carbon contents and the smaller α grain sizes of the hot-rolled material. As the amount of CR increases, the α grains develop a fibrous structure, with the ⟨110⟩ crystallographic direction parallel to the rolling direction, thus providing an unfavorable texture for deep drawing operations. At the same time, the γ fibers lie with their {111} planes parallel to the rolling plane, a

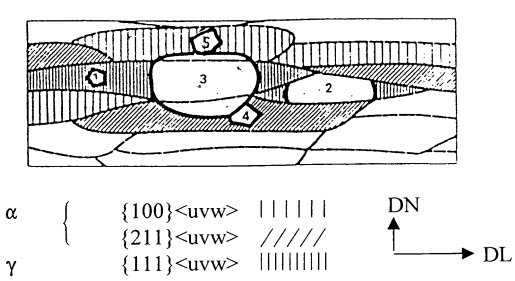

Fig. 11. A schematic representation of the recrystallization process of a cold-rolled ferritic.

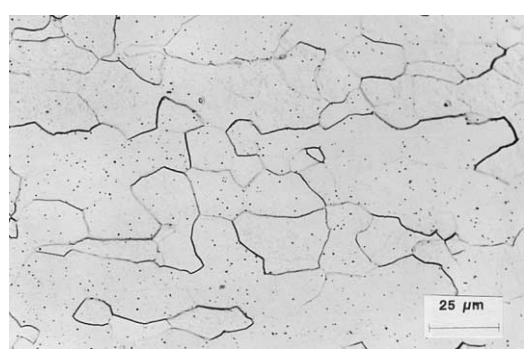

Fig. 12. Microstructure of the IF steel in the cold-rolled and annealed condition. Etchant: 2% Nital.

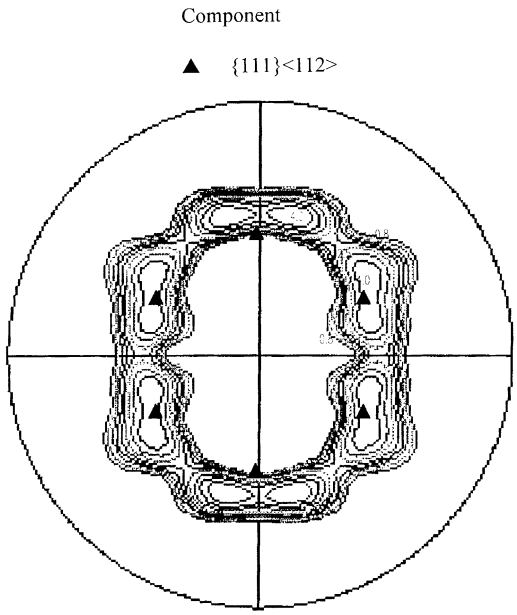

Fig. 13. {200} Pole figure of the IF steel in the cold-rolled and annealed condition.

condition favorable for deep drawing and, in particular, one that yields high Δr values. The simplified ratio $I_{\{100\}}/I_{\{111\}}$, often interpreted as the ratio of α texture to γ texture, increases with the percentage of CR during rolling to 70%, independent of the C content. For reductions to a higher level, it is possible to discern two markedly different behaviors in the steels in the present study.

3.2.1. Tinplate steels and conventional autobody steels

Tinplate steels and autobody steels are produced with CRs of the order of 70% in allowing high r_m values in the annealed sheet. Fig. 7 is a micrograph of a longitudinal cross section of the tinplate steel in the cold-rolled and annealed condition. The α grains have a pancaked structure, and there is carbide precipitation in abundance, showing a general alignment with the rolling direction. Fig. 8 shows the pole figure of this steel with the two principal components for good deep drawability: {111}⟨112⟩ and {111}⟨110⟩.

Fig. 9 is an example of the microstructure, in the longitudinal cross section, of the autobody steel. As with the tinplate steel of Fig. 7, it is characterized by pancaked grains of similar size and abundant coarse cementite precipitation. The {111}⟨112⟩ and {111}⟨110⟩ texture components, associated with good deep drawability, are evident in Fig. 10. This pole figure shows a pattern similar to that found in the tinplate steel (Fig. 8).

Table 3 summarizes the principal texture components of the autobody steel samples after CR and after subsequent annealing and temper rolling (TR). The values in the table are compared intensities, using isotropic sheet steel as the reference material. Two cold reduction states are shown, 70% and 90%, with each state later batch annealed at 50–700 °C/h, then held for 1 and 3 h.

Following the CR, the presence of the principal texture components of the α fibers, γ fibers, and also neighboring ones such as the {554}⟨225⟩ orientation was observed. The observations made also show that, as the degree of CR increased, so did the compared intensities of the various components. After annealing, intensification of the γ fiber texture at the expense of α texture was noted, particularly in samples deformed by 70%. However, some grains with α fiber texture (such as the {001}⟨110⟩ and {112}⟨110⟩ orientations) could still be detected in the 90% cold-deformed material after annealing. As has been noted earlier, the {001}⟨110⟩ texture component results in poor drawability. This means that, despite the fact that the texture in the sheet is primarily γ, the presence of some grains with this unfavorable texture is sufficient to down-rate the overall quality to the DQ level. Through a nucleation and growth model [8], it is explained under some circumstances that the α drawing textures may not fully disappear. In effect, this model is based on the oriented nucleation and

Table 4
Principal texture components of an IF steel after CR and after CR plus batch annealing

	CR		CR and annealing	
Texture	CR = 70%	CR = 90%	CR = 70%; $T_a(\cdot)$ = 50 °C/h); T_a = 700 °C; t_a = 1 h	CR = 90%; $T_a(\cdot)$ = 50 °C/h); T_a = 700 °C; t_a = 3 h
{001}⟨110⟩	4.75	16.46	0.83	0.00
{112}⟨110⟩	3.24	16.42	4.52	1.01
{223}⟨110⟩	3.23	17.07	7.15	6.95
{111}⟨110⟩	2.67	8.47	7.59	9.00
{111}⟨112⟩	3.32	9.78	6.89	20.15
{554}⟨225⟩	4.88	6.30	10.65	22.38
{556}⟨395⟩	3.67	11.12	7.98	29.26

Table 5
Values of r_m and Δr for the most common orientations in steels for cold drawing operations (from Ref. [8])

Crystalline orientation	r_m	Δr
$\{100\}\langle 011\rangle$	0.4	−0.8
$\{112\}\langle 011\rangle$	2.1	−2.7
$\{111\}\langle 011\rangle$	2.6	0.0
$\{111\}\langle 112\rangle$	2.6	0.0
$\{554\}\langle 225\rangle$	2.6	1.1

growth of grains with $\{111\}\langle uvw\rangle$ texture at the expense of grains with α texture or neighboring ones such as the $\{211\}\langle uvw\rangle$ and $\{100\}\langle uvw\rangle$ textures. This is illustrated in Fig. 11. The grains numbered 1, 2 and 3 have a γ texture, so they nucleate and grow rapidly, consuming the unrecrystallized grains. However, the grains numbered 4 and 5 possess an α texture and, since they store less energy of deformation, their recrystallization and growth kinetics are retarded. The extent to which these grains remain in the cold-rolled and annealed state is determined by the capacity for preferential growth of γ grains over grains with a $\{100\}\langle uvw\rangle$ texture.

3.2.2. Interstitial-free steel

With the IF steels, it is desirable to achieve higher CRs because the texture relationship $\{100\}/\{111\}$ decreases as the CR is gradually increased from 70% to 90%. This fact reveals the particular influence of chemical composition, microstructure and texture of the hot-deformed sheet, and lastly of the reduction percentage applied during cold rolling towards the high drawability ranges.

Fig. 12 shows the microstructure of an IF steel after 90% CR and annealing at 700 °C for 3 h. The grain size is rather heterogeneous, with the presence of small grains in the range 10–20 μm, the boundaries of which are preferentially etched. A homogeneous TiC precipitation can also be seen throughout the microstructure, but this does not contribute to hardening of the material.

The $\{200\}$ pole figure is shown in Fig. 13, and it is nominally similar to that of the tinplate and autobody sheet steels after cold rolling and annealing (Figs. 8 and 10, respectively). The $\{111\}\langle 112\rangle$ texture is the only orientation plotted in Fig. 13. Table 4 indicates the development of a new orientation, $\{556\}\langle 395\rangle$, similar to a γ fiber because of its vicinity, with a very strong intensity. IF steels produced according to the specified processing parameters (90% CR, 700 °C/3 h, 50 °C/h) allowed the attainment of an optimum in the cold deformation parameters: $r_m = 2.4$, $\Delta r \approx 0$ and $n > 0.25$. This combination of parametric values corresponds to an EDDQ, and, to our knowledge, represents a "ceiling" for the maximum formability grade that can be obtained in ferritic steels. For comparison, Table 5 summarizes the values of r_m and Δr calculated for monocrystals with orientations typical of deformed and/or recrystallized microstructures in ferritic mild steels for sheet metal forming [7].

4. Conclusions

The results reported in the previous sections enable us to draw the following conclusions.

(1) The processing of steel for cold-forming operations should be subordinated to the DQ requested. Such quality depends on the chemical composition, the microstructure and texture of the hot-rolled strip, the percentage of CR, the annealing process (batch or continuous annealing) and the coiling temperature after hot rolling.

(2) DQ steels are associated with high values for r_m and small Δr values. This level is particularly suitable for the continuous annealing lines, after "hard" hot-rolling schedules and CRs of 70%.

(3) DDQ steels are associated with high r_m values and also unavoidably high Δr values. It must be emphasized that the $\{554\}\langle 255\rangle$ texture component initiates ear formation at 0° and 90° to the rolling direction. Generally, fabrication of such steels is based on the application of "moderate" hot-rolling schedules and CRs of approximately 70%. The process can be adapted to existing annealing facilities for recrystallization.

(4) Steels of EDDQ, with r_m values higher than 2, require process modifications if the goal is the minimization of the planar anisotropy of the sheet (the Δr value). The use of "soft" hot-rolling schedules with finishing passes below the allotropic $\gamma \rightarrow \alpha$ transformation temperature, followed by heavy CR (90%) and finishing with batch annealing, is suggested. It must be pointed out that this results in the appearance of a novel $\{556\}\langle 395\rangle$ texture component that counteracts the former $\{554\}\langle 225\rangle$ component. As a result, the sheet behaves in an almost fully isotropic manner in the rolling plane.

(5) It is concluded that the recrystallization process is initiated and developed through a mechanism of oriented nucleation and growth. This has given rise to the development of cold-rolled sheet in which the highest proportion of grains has a $\{111\}\langle uvw\rangle$ texture, favorable for deep drawing operations.

Acknowledgments

The authors express their gratitude to Mr. C. Alonso of Aceralia Corporacion Siderurgica for the

experimental material and related information. Many thanks are also due to Dr. C. Rosales and Dr. J. Gil-Sevillano of the CEIT, for their help in the preparation of the experimental part and valuable discussions in the elaboration of this paper.

References

[1] Pickering FB. Physical metallurgy and the design of steels. London, UK: Applied Science Publishers, 1993 (Materials Science Series).

[2] Pero-Sanz JA. Ciencia e Ingeniería de Materiales. 4th ed. Madrid: Dossat 2000, 1999 (in Spanish).

[3] Lewellyn DT. Steels: metallurgy and applications. London, UK: Butterworths, 1995.

[4] Lévy J. Introduction à la Métallurgie générale. Paris, France: Ed. Les Presses E.M.P, 1999.

[5] Barbosa R, Boratto F, Yue S, Jonas JJ. The influence of chemical composition on the recrystallization behavior of microalloyed steels. Proceedings of the International Conference on Processing Microstructure and Properties of HSLA Steels. Pittsburgh (PA): The Mineral, Metals and Materials Society, 1987. pp. 51–6.

[6] Verdeja, JI. Le chiffonnage des alliages Fe–17%Cr et Fe–3%Si. PhD thesis, University of Paris, Paris, France, 1978.

[7] Ray RK, Jonas JJ, Hook RE. Cold rolling and annealing textures in low carbon and extra low carbon steels. Int Met Rev 1994;39(4):129–72.

[8] Parnière P. Recrystallization textures of low carbon steel sheets. Proceedings of the 6th International Conference on Texture of Materials. Tokyo (Japan): Iron and Steel Institute of Japan, 1981. pp. 181–94.